Neuro-Oncology 15(12):1604–1614, 2013.
doi:10.1093/neuonc/not132

Activation of mTORC1/mTORC2 signaling in pediatric low-grade glioma and pilocytic astrocytoma reveals mTOR as a therapeutic target

Marianne Hütt-Cabezas, Matthias A. Karajannis, David Zagzag, Smit Shah, Iren Horkayne-Szakaly, Elisabeth J. Rushing, J. Douglas Cameron, Deepali Jain, Charles G. Eberhart, Eric H. Raabe, and Fausto J. Rodriguez

Division of Neuropathology and Sidney Kimmel Comprehensive Cancer Center, Johns Hopkins University, Baltimore, Maryland (M.H.-C., S.S., D.J., C.G.E., E.H.R., F.J.R.); Division of Pediatric Oncology, Johns Hopkins University, Baltimore, Maryland (E.H.R.); Division of Pediatric Hematology/Oncology, Department of Pediatrics, NYU Langone Medical Center, New York, New York (M.A.K.); Division of Neuropathology, Department of Pathology and Neurosurgery, NYU Langone Medical Center, New York, New York (D.Z.); Joint Pathology Center, Silver Spring, Maryland (I.H-S.); Institute of Neuropathology, University Hospital Zurich, Zurich, Switzerland (E.J.R.); Department of Ophthalmology, Department of Laboratory, and Department of Medicine and Pathology, University of Minnesota, Minneapolis, Minnesota (J.D.C.)

Background. Previous studies support a role for mitogen-activated protein kinase pathway signaling, and more recently Akt/mammalian target of rapamycin (mTOR), in pediatric low-grade glioma (PLGG), including pilocytic astrocytoma (PA). Here we further evaluate the role of the mTORC1/mTORC2 pathway in order to better direct pharmacologic blockade in these common childhood tumors.

Methods. We studied 177 PLGGs and PAs using immunohistochemistry and tested the effect of mTOR blockade on 2 PLGG cell lines (Res186 and Res259) in vitro.

Results. Moderate (2+) to strong (3+) immunostaining was observed for pS6 in 107/177 (59%) PAs and other PLGGs, while p4EBP1 was observed in 35/115 (30%), pElF4G in 66/112 (59%), mTOR (total) in 53/113 (47%), RAPTOR (mTORC1 component) in 64/102 (63%), RICTOR (mTORC2 component) in 48/101 (48%), and pAkt (S473) in 63/103 (61%). Complete phosphatase and tensin homolog protein loss was identified in only 7/101 (7%) of cases. In PA of the optic pathways, compared with other anatomic sites, there was increased immunoreactivity for pS6, pElF4G, mTOR (total), RICTOR, and pAkt ($P < .05$). We also observed increased pS6 ($P = .01$), p4EBP1 ($P = .029$), and RICTOR ($P = .05$) in neurofibromatosis type 1 compared with sporadic tumors. Treatment of the PLGG cell lines Res186 (PA derived) and Res259 (diffuse astrocytoma derived) with the rapalog MK8669 (ridaforolimus) led to decreased mTOR pathway activation and growth.

Conclusions. These findings suggest that the mTOR pathway is active in PLGG but varies by clinicopathologic subtype. Additionally, our data suggest that mTORC2 is differentially active in optic pathway and neurofibromatosis type 1–associated gliomas. MTOR represents a potential therapeutic target in PLGG that merits further investigation.

Keywords: mTOR, neurofibromatosis, optic nerve, pediatric glioma, pilocytic astrocytoma.

Pediatric low-grade gliomas (PLGGs) represent the most common group of tumors involving the central nervous system in children.[1] Although they are characterized by slow growth and a low frequency of malignant progression, morbidity may be considerable, particularly when located in anatomic regions not amenable to surgical resection. Traditional therapies, such as irradiation and conventional chemotherapy,

Received May 23, 2013; accepted July 18, 2013.

Corresponding Authors: Fausto J. Rodriguez, MD, Division of Neuropathology, Johns Hopkins Hospital, 1800 Orleans Street, Baltimore, MD 21231 (frodrig4@jhmi.edu; eraabe2@jhmi.edu); Eric H. Raabe, MD, PhD, Division of Neuropathology, Johns Hopkins Hospital, 1800 Orleans Street, Baltimore, MD 21231 (eraabe2@jhmi.edu)

are not curative and often fail in preventing clinical progression.

The most common low-grade glioma in children is pilocytic astrocytoma (PA), a World Health Organization grade I tumor with low proliferative potential. Until recently, little was known about the biology of PLGG. In PA arising in patients with neurofibromatosis type 1 (NF1), there is inactivation of both *NF1* gene copies,[2] leading to hyperactive Ras and downstream mitogen-activated protein kinase (MAPK) pathway activation. More recently, independent high resolution genomic studies have identified a tandem duplication of *BRAF* at 7q34 in the majority (53%–72%) of PAs leading to an oncogenic fusion gene.[3–6] In a smaller proportion of cases, *BRAF* activating point mutations and rearrangements of other *BRAF* family members (eg, *RAF1*) may also be encountered.[7] These alterations seem to vary by anatomic site, with the highest frequency of *BRAF* duplications occurring in PA of the cerebellum.[8] However, a recent study using archival material from tumors of the optic nerve proper showed that the majority of tumors (73%) also had duplications of the *BRAF* kinase domain, with the remainder being associated with NF1.[9] These genetic aberrations share an increased MAPK/extracellular signal-regulated kinase pathway activation, which is active in the majority of PAs. More recent whole genome sequencing efforts of PLGG and PA have found that these neoplasms are characterized in many cases by single somatic mutations, with pediatric diffuse low-grade gliomas containing alterations in *FGFR1*, *MYB*, or *MYBL1*.[10,11]

The phosphatidylinositol-3 kinase (PI3K)/Akt/mammalian target of rapamycin (mTOR) pathway is active in a variety of cancers, and effective pharmacologic inhibitors such as rapamycin and analogs (rapalogs) are widely available. The importance of the PI3K/Akt/mTOR signaling axis has been highlighted in diffuse and high-grade gliomas.[12] One of the key downstream mediators of PI3K/Akt activation is mTOR, which exists in 2 complexes: mTORC1 and mTORC2, which possess distinct regulatory inputs and outputs within the signaling network (Fig. 1). In the mTORC1 complex, mTOR interacts with proline rich Akt substrate, 40 kDa; regulatory associated protein of mTOR, complex 1 (RAPTOR); and mammalian lethal with SEC13 protein 8 (mLST8)/G protein beta subunit-like (GBL), and upon activation increases protein translation, cell growth, and survival. The function of the mTORC2 complex (mTOR, rapamycin-insensitive companion of mTOR [RICTOR], mSin1, Protor [protein observed with Rictor], and mLST8) is less well known, but it appears to regulate metabolism and survival through activation of Akt, as well as mTORC1, through protein kinase C, and also plays a role in cytoskeletal organization.[13]

Of interest, recent studies have highlighted a role for mTOR activation in NF1-associated PA and murine models of NF1–optic nerve glioma.[14] Recent data also suggest that it may mediate phenotypic variations in NF1-associated low-grade gliomas,[15] with its activation more frequent in the rare PA with anaplastic features.[16] Furthermore, recent evidence suggests that mTOR also mediates the proliferative activity of cerebellar murine stem cells expressing *BRAF* fusions.[17] Of therapeutic relevance, mTOR inhibition has proven to be of great clinical benefit and is well tolerated in pediatric patients with subependymal giant cell astrocytoma, another subtype of PLGG.[18] A possible role for mTOR signaling in the biology of the most common PLGG, that is, sporadic PA, is of interest, given the abundance of pharmacologic data with mTOR inhibitors in a variety of tumor types. Therefore, we decided to investigate the effects of MK8669 (ridaforolimus) in PLGG-derived cell lines.

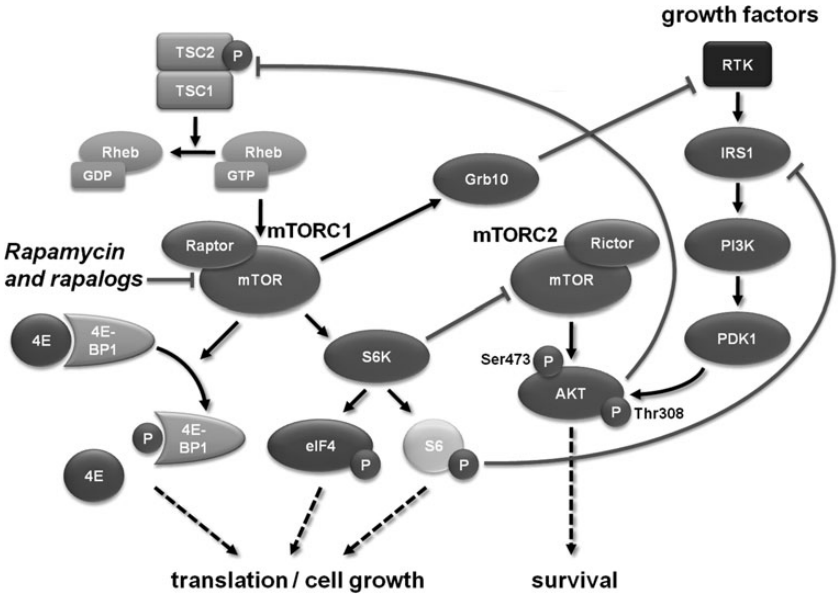

Fig. 1. mTOR pathway signaling cascade. The mTOR pathway exists as part of either of 2 multiprotein complexes (mTORC1 and mTORC2), which are integral components of a signaling cascade that leads to increased cell growth and survival.

Materials and Methods

Patients and Tumor Samples

A total of 63 PLGGs of various histologies were retrospectively studied using whole tissue sections of a representative block (age range, 22 mo–19 y; median, 8 y). An additional 133 PAs were studied using 2 separate tissue microarrays containing 2–4 cores per tumor constructed at the Johns Hopkins Hospital or the former Armed Forces Institute of Pathology as previously reported.[9] Patients' age ranged from 3 months to 66 years (median, 8 y), with 59 females and 74 males. A total of 10 cases (9%) were NF1 associated. A total of 83 cases arose in the optic pathways, with 58 developing in the optic nerve proper; 88 were located in non–optic pathway locations, predominantly in the infratentorial compartment. In the sporadic group with detailed location data, excluding pleomorphic xanthoastrocytomas (PXAs) and oligodendrogliomas, 58 were midline tumors (chiasm, hypothalamus, thalamus, brainstem) and 82 were cerebellar/hemispheric. All studies were performed under appropriate institutional review board approval of all institutions involved.

Immunohistochemistry

Immunohistochemical studies were performed in formalin-fixed/paraffin-embedded tissue microarrays. Primary antibodies included phospho-S6 (Ser235/236) (1:50, rabbit monoclonal; clone 91B2, Cell Signaling), mTOR (total) (1:50, rabbit monoclonal; clone 7C10, Cell Signaling), phospho-4EBP1 (Thr37/46) (1:100, rabbit monoclonal; clone 236B4, Cell Signaling), phospho-ElF4G (Ser1108) (1:400, rabbit polyclonal; Cell Signaling), RAPTOR (total) (1:95, rabbit monoclonal; clone EP539Y, Abcam), RICTOR (total) (1:950, mouse monoclonal; clone 7B3, Abcam), phospho- Akt (Ser473) (1:50, rabbit polyclonal, Cell Signaling), and phosphatase and tensin homolog (PTEN; total) (1:50, rabbit monoclonal; clone D4.3, Cell Signaling). Omission of the secondary antibody was used as the negative control. Scoring of pS6 staining on whole tissue sections was performed by 2 independent observers (D.Z. and F.J.R.), while scoring on tissue microarray sections was performed by a single observer (F.J.R.). A 4-tiered scale was used based on the percentage of tumor cells showing significant (moderate to marked) immunoreactivity: 0 = negative/rare positive cells, 1 = 1%–10% positive cells, 2 = 10%–50% positive cells, and 3 = ≥50% positive cells. Nontumor cells, such as endothelial cells and reactive or entrapped astrocytes, were excluded from scoring.

BRAF-KIAA1549 *and* BRAF *(V600E)*

BRAF-KIAA1549 fusion and *BRAF* (V600E) point mutation data were available for a subset of cases as part of a previously published study.[19] In brief, screening for *BRAF-KIAA1549* variants was performed by polymerase chain reaction (PCR). Primer sequences were as follows: 5′-CGGAAACACCAGGTCAACGG-3′ (*KIAA1549* exon 15, forward) and 5′-GTTCCAAATGATCCAGATCCA ATT-3′ (*BRAF* exon 11, reverse) as previously reported.[4] For *BRAF* (V600E), PCR was performed with exon 15 primers (5′-TCATAATGCTT-GCTCTGATAGGA-3′ (forward) and 5′-GGCCAA-AAATTTAATCAGTGGA-3′ (reverse), followed by Sanger sequencing.

Cell Culture and Drug Treatment

The cell lines used in this study were Res186 and Res259, kindly provided by Dr Chris Jones (Institute of Cancer Research, Sutton, UK).[20] All cell lines were grown in monolayers in Dulbecco's modified Eagle's medium/F12 Ham's medium containing 10% fetal bovine serum and 1% penicillin-streptomycin in a humidified 37°C incubator with 5% CO_2. All cells were verified to be *Mycoplasma* free by PCR testing. MK8669 (ridaforolimus) was kindly provided by Merck. MK8669 was dissolved in dimethyl sulfoxide (DMSO), and 10-mM stocks were stored at −80°C. To decrease the influence of serum on mTOR pathway activation, cells were treated with MK8669 or DMSO control in medium containing 2% fetal bovine serum.

MTS Assay of Cell Growth

Cell growth was examined by assay by MTS (3-(4,5-dimethylthiazol-2-yl)-5-(3-carboxymethoxyphenyl)-2-(4-sulfophenyl)-2H-tetrazolium) using the cell titer 96 Aqueous One solution cell proliferation assay kit (Promega). Twenty microliters of the MTS reagent was added per 100 μL medium in 96-well plates and incubated for 1 h at 37°C in 5% CO_2. Cells were trypsinized, and viable cells were manually counted for plating. Fifteen hundred cells per well were plated in triplicates for reading days 0, 2, 4, and 6 for each condition: DMSO (vehicle), 1 nm MK8669, and 10 nM MK8669. The 490-nm absorbance values were measured using the Epoch Micro-Volume Spectrophotometer Plate Reader System (Biotek) and were directly proportional to the number of viable cells in culture.

Bromodeoxyuridine Incorporation Assay

During the last 6 h of a 48-h incubation, cells were pulsed with 100 μM 5-bromo-2′-deoxyuridine (BrdU; Sigma-Aldrich). Cells were taken out of BrdU-containing medium, made single cells, washed with phosphate buffered saline (PBS), and fixed with methanol at 4°C overnight. Cells were cytospun into Plus slides (Fisher) and processed for BrdU detection.[21] Cells were fixed with 4% paraformaldehyde, washed with PBS containing 0.1% Tween 20 (PBST), permeabilized with 0.1% Triton X-100 in PBST, and washed with PBST. DNA was denatured by incubating with 2N HCl at 37°C, washed again with PBST, and blocked with 5% normal goat serum (NGS) in PBST. Slides were incubated with anti-BrdU primary antibody for 1 h at 37°C at a 1:500

dilution in 5% NGS PBST, washed 3 times with 1X PBST, and incubated with Cy-3 anti-mouse secondary at a 1:500 concentration in 5% NGS PBST for 45 min at 37°C. Cells were finally counterstained with 4′,6′-diamidino-2-phenylindole and coverslipped with antifade mounting media (Vectashield). Results were analyzed in Adobe Photoshop, where BrdU-positive cells were counted using the count tool.

Western Blotting

Cells at 90% confluence were scraped, pelleted, washed with ice-cold PBS, and pelleted at 4°C. Pellets were lysed with chilled radioimmunoprecipitation assay 2 buffer (20 mM Tris, pH 7.4; 10% glycerol; 137 mM NaCl; 0.1% sodium dodecyl sulfate; 1% Triton X-100; 2 mM EDTA; 0.5% sodium deoxycholate) supplemented with 10 mM sodium fluoride, 1 mM sodium vanadate (Cell Signaling Technology), Roche protease inhibitor cocktail, and phenylmethylsulfonyl fluoride (Sigma-Aldrich). Fifty micrograms of lysate for each sample per lane was run in precast NuPAGE Novex polyacrylamide gel 4%–12% Bis-Tris Gels (1.0-mm thick, 10-well) in 1X Tris-glycine. Lysates were transferred onto a nitrocellulose membrane (Bio-Rad), blocked in PBS containing 5% bovine serum albumin or nonfat dry milk powder, and incubated overnight with antibodies per manufacturer's directions. Blots were then washed several times with PBS containing 0.1% Tween 20 and incubated in peroxidase-conjugated immunoglobulin G diluted 1:5000 in blocking solution. After washing several times in PBS with 0.1% Tween 20, blots were developed with enhanced Western Lightning electrochemiluminescence reagent (Perkin Elmer) and exposed to film. Primary antibodies included phospho-S6 (Ser235/236) (1:1000, rabbit monoclonal; Cell Signaling), phospho-Akt (Ser473) (1:1000, rabbit monoclonal; Cell Signaling), Akt (pan) (1:1000, rabbit monoclonal; C7E7, Cell Signaling), S6 ribosomal protein (1:1000, mouse monoclonal; 54D2, Cell Signaling), anti–glyceraldehyde-3-phosphate dehydrogenase (1:500 000; clone 6C5, Research Diagnostics), and β-actin (1:500; C4, Santa Cruz Biotechnology). Omission of the secondary antibody was used as the negative control.

Statistical Analyses

For immunohistochemical and survival analyses, variables were described using proportions, ranges, and medians as appropriate. Fisher's exact tests were used to compare proportions, and Student's *t*-test or Wilcoxon rank sum was used to compare continuous variables between groups of interest. Survival rates were described using Kaplan–Meier curves and analyzed with the log-rank test. The time to event was defined as time from surgery to death/tumor progression (or last follow-up if censored). Statistical analyses were performed using JMP v10 software (SAS Institute). Analyses were 2-sided with $P < .05$ considered statistically significant. For in vitro assays, statistical significance was determined by using GraphPad Prism Software ($^{**}P < .01$, $^{***}P < .001$). Multiple comparisons were performed by ANOVA with Tukey correction. Error bars represent the standard deviation for all plots.

Results

Activation of mTORC1 Pathway Is Frequent in Pediatric Low-Grade Glioma

Using whole tissue sections, pS6 reactivity of any degree of tumor cells was seen in 56/62 (90%) of PLGGs of various histologic types. Moderate to strong (2–3) immunostaining for pS6 was present in 39 (63%), including 25/36 PAs (69%) , 5/8 PXAs (63%), 2/2 diffuse astrocytomas, 2/2 astrocytomas with pilomyxoid features, and 5/8 (63%) unclassifiable low-grade astrocytomas. Pediatric oligodendrogliomas ($n = 6$) showed weak to absent pS6 staining in all cases tested. There was a trend for lower pS6 staining in tumors with *BRAF-KIAA1549* fusions (16/27 [59%] with moderate to marked pS6 vs 26/34 [77%] in tumors without *BRAF-KIAA1549*), although this did not reach statistical significance ($P = .17$, Fisher's exact test). Findings are summarized in Table 1 and illustrated in Fig. 2. To further confirm the activation of mTORC1 in PA, we analyzed protein lysates from frozen primary tumors. Increased pS6 levels were identified by Western blot in 4 primary pediatric PAs compared with nonneoplastic pediatric brain (Supplementary Fig. S1).

Immunoreactivity for mTORC1/mTORC2 Pathway Components Is Frequent in PA

Because PA is the most frequent PLGG, we systematically studied PAs in tissue microarrays representing different anatomic sites, including optic pathways ($n = 83$) and infratentorial/supratentorial compartments ($n = 58$), for mTOR signaling components. Moderate (2+) to strong (3+) immunostaining was observed for mTORC1 components pS6 in 67/113 (59%), p4EBP1 in 35/115 (30%), pEIF4G in 66/112 (59%), mTOR (total) in 53/113 (47%), and RAPTOR (total) in 64/102 (63%). The majority of tumors with p4EBP1 immunoreactivity had pS6 reactivity as well (94%). Activation of mTORC2 component pAkt (S473) was present in 63/103 (61%), and RICTOR (total) was detected in 48/101 (48%). Almost all (98%) tumors with pAkt immunoreactivity were also pS6 positive, while 12% of pS6-positive tumors were completely pAkt negative. Conversely, there was no difference in mTORC1/mTORC2 component immunoreactivity when comparing sporadic midline ($n = 58$) with sporadic cerebellar/hemispheric tumors ($n = 82$; $P > .05$). In summary, combined mTORC1 and mTORC2 activation of any degree was present in 81% of tumors based on pS6 and pAkt immunoreactivity, and this was significant (moderate to strong) in 46%. Conversely, complete PTEN protein loss was identified in only 7/101 (7%).

Table 1. Frequency of moderate (2+) to marked (3+) immunoreactivity for mTOR pathway components in PA and PLGA

Marker N/total scorable (%)	Sporadic PA	NF1-associated PLGA	Optic pathway PA	Non–optic pathway PA	Pediatric PA	Adult PA	PLGA With BRAF-KIAA1549	PLGA With BRAF (V600E)	PA With Pilomyxoid Features	Pediatric DA (grade II)	Pediatric PXA (grade II)	PLGA NOS	Ped Oligo (grade II)	Total
Phosho-S6*	68/119 (57)	10/11 (91)	53/75 (71)	38/72 (53)	82/132 (62)	11/19 (58)	16/27 (59)	3/4 (75)	2/2 (100)	2/2 (100)	5/8 (63)	5/8 (63)	0	107/177 (59)
Phospho-4EBP1	21/83 (25)	5/9 (56)	25/66 (38)	10/49 (20)	30/96 (31)	5/19 (26)	NA	NA	NA	NA	NA	NA	NA	35/115 (30)
phospho-EIF4G	43/81 (53)	6/9 (67)	46/64 (72)	20/48 (42)	56/94 (60)	10/18 (56)	NA	NA	NA	NA	NA	NA	NA	66/112 (59)
mTOR (total)	34/82 (41)	4/8 (50)	35/65 (54)	18/48 (38)	49/97 (51)	4/16 (25)	NA	NA	NA	NA	NA	NA	NA	53/113(47)
RAPTOR (total)	42/71 (59)	5/7 (71)	43/64 (67)	21/38 (55)	55/90 (61)	9/12 (75)	NA	NA	NA	NA	NA	NA	NA	64/102 (63)
RICTOR (total)	27/74 (36)	5/6 (83)	41/62 (66)	7/39 (18)	39/88 (44)	9/13 (69)	NA	NA	NA	NA	NA	NA	NA	48/101 (48)
phospho-Akt (S473)	44/73 (60)	6/6 (100)	44/63 (70)	19/39 (49)	55/88 (63)	8/14 (57)	NA	NA	NA	NA	NA	NA	NA	63/103 (61)
PTEN	57/71(80)	6/6 (100)	51/64 (80)	28/36 (78)	73/87 (84)	6/13 (46)	NA	NA	NA	NA	NA	NA	NA	80/101 (79)

Abbreviations: DA, diffuse astrocytoma; NOS, not otherwise specified; NA, not available.
*Performed on whole sections and tissue microarray sections.

Immunoreactivity for mTOR Pathway Components Is Stronger in Optic Pathway and NF1-Associated PA

Next we looked for differences in immunoreactivity of mTOR components by anatomic site and NF1 association, factors previously associated with distinct gene expression patterns and tumor biology.[22] There was increased immunoreactivity in PAs of the optic pathways compared with other anatomic sites for mTORC1 components pS6 ($P = .02$), pElF4G ($P = .0003$), mTOR (total) ($P = .02$), and mTORC2 components RICTOR ($P = .0001$) and pAkt (S473) ($P = .02$, Wilcoxon rank sum; Fig. 3). Conversely, there was no difference by site for p4EBP1 ($P = .28$), RAPTOR ($P = .15$), or PTEN ($P = .68$) immunoreactivity. NF1-associated tumors demonstrated increased pS6 ($P = .01$), p4EBP1 ($P = .029$), and RICTOR ($P = .05$) compared with non-NF1 tumors. There was a trend toward increased pAkt (S473) ($P = .07$) in these syndromic cases, but no difference for pElF4G, mTOR, RAPTOR, or PTEN immunoreactivity ($P > .05$).

Components and Outcome of mTOR Pathway

There was improved recurrence-free survival in patients with infratentorial PAs, predominantly cerebellar, compared with optic pathway and supratentorial tumors ($P = .03$), as well as those who underwent gross total resection ($P < .001$). Most tumors that underwent gross total resection were located in the posterior fossa (cerebellum/4th ventricle; 26/32 [81%]) or were hemispheric (4/32 [13%]). There was no association between strong immunoreactivity for mTOR pathway components and recurrence-free survival.

MK8669 Inhibits the PI3K/Akt/mTORC1 Pathway

We measured mTOR pathway activation via Western blot in 2 previously described PLGG cell lines (Res186 and Res259).[20] Both of these lines have active mTORC1/mTORC2 in vitro as measured by phosphorylated ribosomal protein S6 at serine 235/236 and phosphorylated Akt at serine 473, respectively (Fig. 4). To assess whether mTORC1 could be inhibited in these cells, we chose 2 different concentrations of the rapalog MK8669 (ridaforolimus). MK8669 is an allosteric mTORC1 inhibitor that prevents the phosphorylation of ribosomal protein S6, and we observed a dose-dependent decrease in the phosphorylation of S6 with treatment of MK8669 in Res186 and Res259, with a concomitant increase in mTORC2 activation, as measured by phosphorylated Akt473 (Fig. 4A and B).

MK8669 Suppresses Growth of Low-Grade Astrocytoma Cell Lines

To determine the potential clinical effects of mTORC1 blockade, we examined how MK8669 modulated growth of PLGG cells in culture. An MTS assay showed that treatment of Res186 with 1 nM or 10 nM MK8669

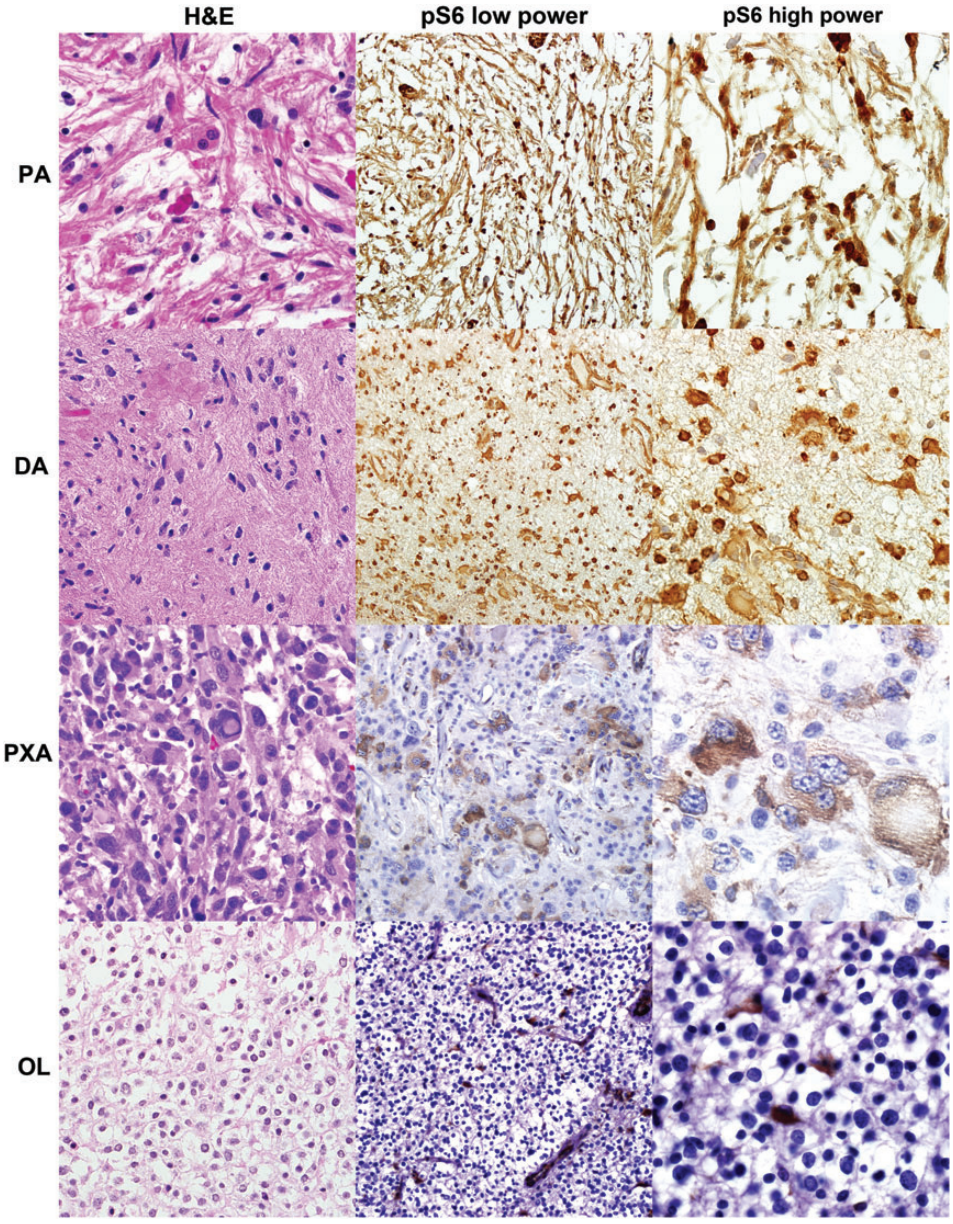

Fig. 2. mTORC1 pathway is active in PLGG. Every category of PLGG tested demonstrated pS6 immunoreactivity, compatible with mTORC1 activation, in a significant subset, including PA, diffuse astrocytoma (DA), and PXA. However, pediatric low-grade oligodendrogliomas (OL) were predominantly negative, except for occasional entrapped/reactive astrocytes.

led to significant reductions (63% or 73%, respectively) in cell growth over 6 days ($P < .0001$, ANOVA; Fig. 5A and B). Res259 showed more modest but still significant decreases in growth after 4 days of treatment with 1 nM MK8669 (13%, $P < .05$, ANOVA)) or 10 nM MK8669, respectively (21%, $P < .0001$, ANOVA) compared with vehicle (Fig. 5C and D).

Treatment With MK8669 Decreases S-phase Entry

BrdU incorporation assays revealed that treating Res186 cells with MK8669 reduces the number of BrdU-positive cells by 66% at the lowest drug concentration of 1 nM MK8669 compared with control ($P = .0046$, ANOVA; Fig. 5E). A trend toward decrease without significance in BrdU positivity was observed in the Res259 cell line when treated with MK8669 ($P = .10$, ANOVA; Fig. 5F). These results suggest that MK8669 decreases cell growth and proliferation in Res186 cells by preventing S-phase entry.

Discussion

In this study, we explored a possible role for the mTOR pathway in PLGG biology and its feasibility as a therapeutic target in vitro. Several prior lines of work suggest that

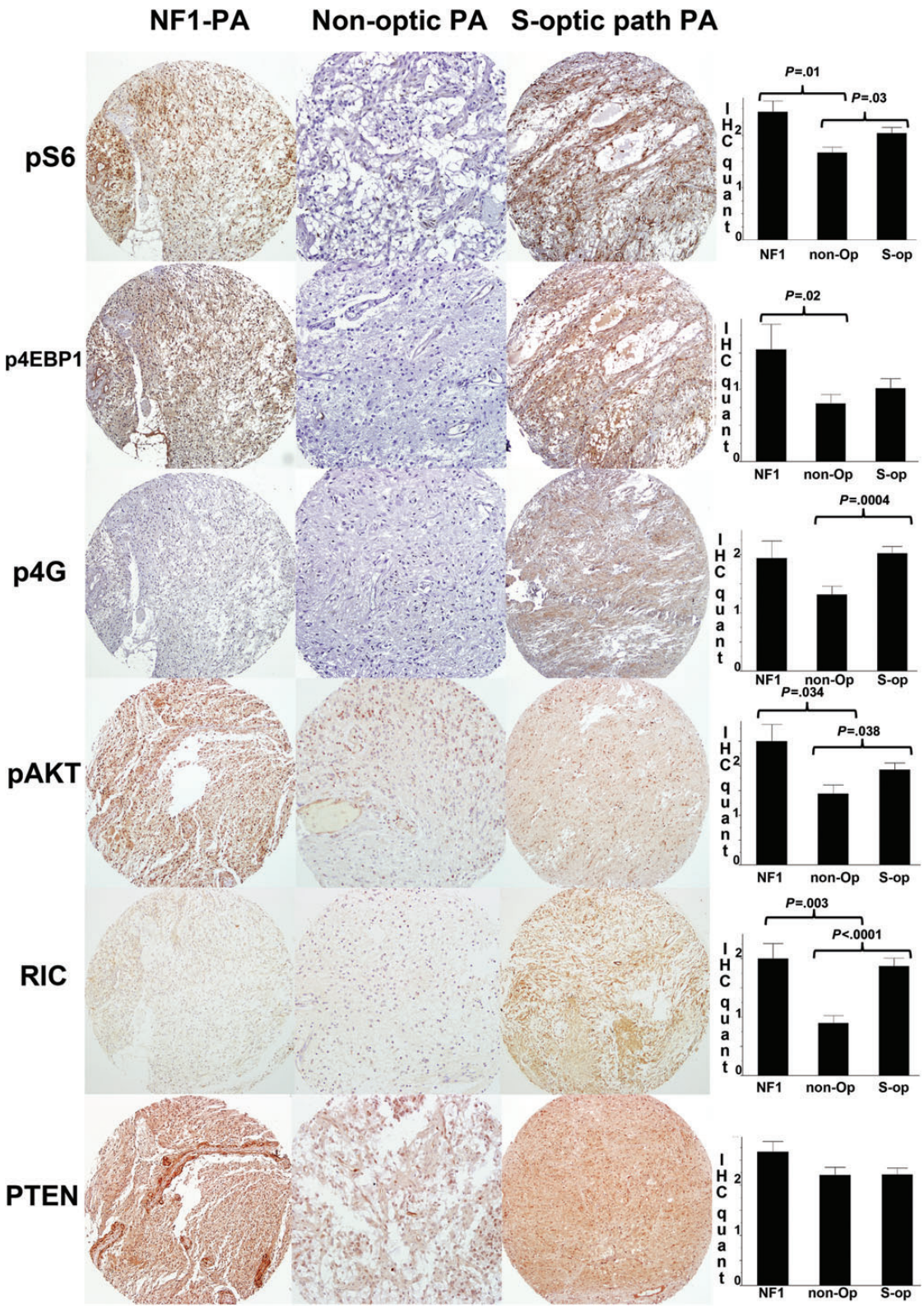

Fig. 3. mTORC1 and mTORC2 pathways are activated to a greater extent in NF1-associated and optic pathway PAs. Immunoreactivity for mTORC1 (pS6, p4EBP1, p4G) and mTORC2 (pAkt [S473], total RICTOR [RIC]) pathway components were more frequent in NF1-associated PAs (NF1PA) and sporadic optic pathway PAs (S-op) compared with non–optic pathway PAs. Semiquantification of immunopositive cells is provided on the right in a scale from 0–3. Only *P*-values for statistically significant comparisons are presented.

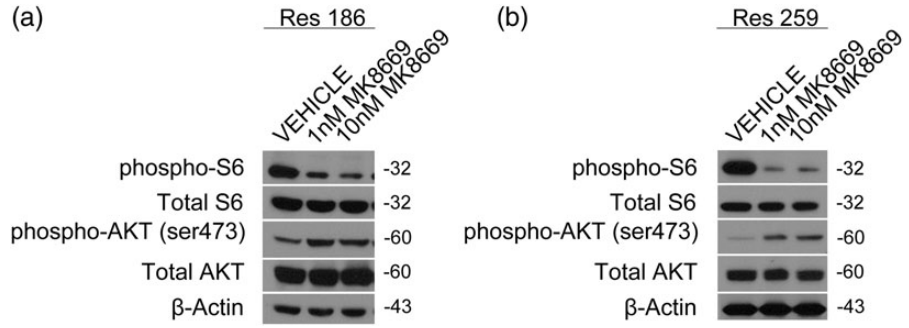

Fig. 4. mTORC1 pathway is inhibited by MK8669 in PLGG cell lines Res186 and Res259. Western blot showing activation levels of mTORC 1/2 (pS6/pAkt473) under normal growth conditions in cell lines Res186 (**a**) and Res259 (**b**). Western blot showing target mTORC1 inhibition (pS6) with a concomitant mTORC2 increase (pAktSer473) using MK8669 in Res186 (**a**), and a similar although modest effect is seen in Res259 low-grade glioma cell line (**b**). Cells in this experiment were grown in media with 2% fetal bovine serum.

mTOR activation may be relevant to PLGG biology. First, neurofibromin loss, a hallmark of NF1-associated PA, leads to astrocyte hyperproliferation, a phenomenon that appears to be related to mTOR activation.[14] In addition, a subset of NF1-associated low-grade gliomas demonstrate increased cell size and macronucleoli, as well as increased immunostaining for markers of mTOR pathway activity.[15] Interestingly, mTOR activation resulting from neurofibromin loss may depend on anatomic location and be secondary to mTORC2 activation.[23] Our study demonstrates increased mTORC2 components pAkt (S473) and total RICTOR levels in NF1-associated low-grade gliomas or PAs of the optic pathways compared with other tumor types. These effects do not appear to be mediated by PTEN loss, and this is further supported by our current study, which showed preserved PTEN immunoreactivity in all NF1-associated low-grade gliomas tested. Subependymal giant cell astrocytoma represents another low-grade, predominantly pediatric, astrocytoma that almost always occurs in the setting of tuberous sclerosis complex, which can serve as a model for this type of targeted therapy given the recent clinical success of mTOR inhibitors.[24] In these tumors, mTOR pathway activation is a direct consequence of loss-of-function mutations of the *TSC1* or *2* tumor suppressor genes, which leads to mTOR activation mediated by Ras homolog enriched in brain (RHEB).[13] We were intrigued that mTOR pathway activation was a feature of the majority of PLGGs in our study, including most grade II tumors, with the exception of pediatric oligodendrogliomas. This finding supports a more dominant role for mTOR pathway signaling in PLGG with astrocytic or neuronal differentiation, compared with the relatively rare pediatric oligodendrogliomas.

A role for mTOR signaling in the biology of PLGG was also highlighted by recent whole genome/exome sequencing efforts. In a recent whole genome sequencing study, *FGFR1* alterations were relatively frequent in nonpilocytic PLGGs.[11] In that study, introduction of *FGFR1* into MCF7 breast cancer cells led to PI3K activation, an effect that was suppressed by an mTOR inhibitor. In a separate study, exome sequencing demonstrated mutations in 4/12 (33%) PXAs affecting genes associated with mTOR pathway activation, including *NF1*, *TSC2*, and *PIK3R1*.[25] Interestingly, these mutations were not found in tumors with the more frequent *BRAF* (V600E) alteration typical of PXA.[26] Since pS6 immunoreactivity was frequent in these tumors in our current study, it is possible that *BRAF* mutations may affect mTOR signaling. For example, we found immunoreactivity for pS6 of any extent in 7/8 PXAs, which was moderate or strong in 5. In addition, we found pS6 immunoreactivity in all 4 tumors with *BRAF* (V600E) tested, which was moderate or strong in 3.

Of greater interest for therapeutic targeting is whether the mTOR pathway is active in sporadic PA, the largest category of PLGG in children. The genetic hallmark of sporadic PA is a somatic *BRAF-KIAA1549* fusion. Although there is experience with BRAF inhibitors as a therapeutic strategy for non-CNS tumors, particularly metastatic melanoma, several important caveats have emerged recently. In particular, most available BRAF inhibitors are effective against BRAF (V600E) mutant tumors but may cause a paradoxical increase in signaling activity and growth in cells containing *BRAF* fusions.[27] This further reinforces prior observations that various genetic alterations associated with increased MAPK pathway activity result in different biologic properties. In our study, we found a nonsignificant trend for lower pS6 immunostaining in tumors containing *BRAF-KIAA1549* compared with tumors lacking it. However, most sporadic PAs tested demonstrated increased pS6 immunostaining, supporting the notion that the mTOR pathway is broadly active in these tumors as well.

Interestingly, recent data by Kaul et al[17] demonstrate that *BRAF-KIAA1549* does indeed lead to neural stem cell proliferation and glioma-like lesions in mice. In their model, this effect appeared to be mediated by RHEB activation resulting from inhibition of TSC1/TSC2 protein complex. These and our results are in keeping with the study published by Mueller et al,[28] who demonstrated mTOR pathway activation in both pediatric high-grade and low-grade gliomas. In contrast to our series, that study was limited to 25 grade I and 7 grade II PLGGs and in regard to specific mTOR readout was limited to pS6 and p4EBP1. Mueller et al also

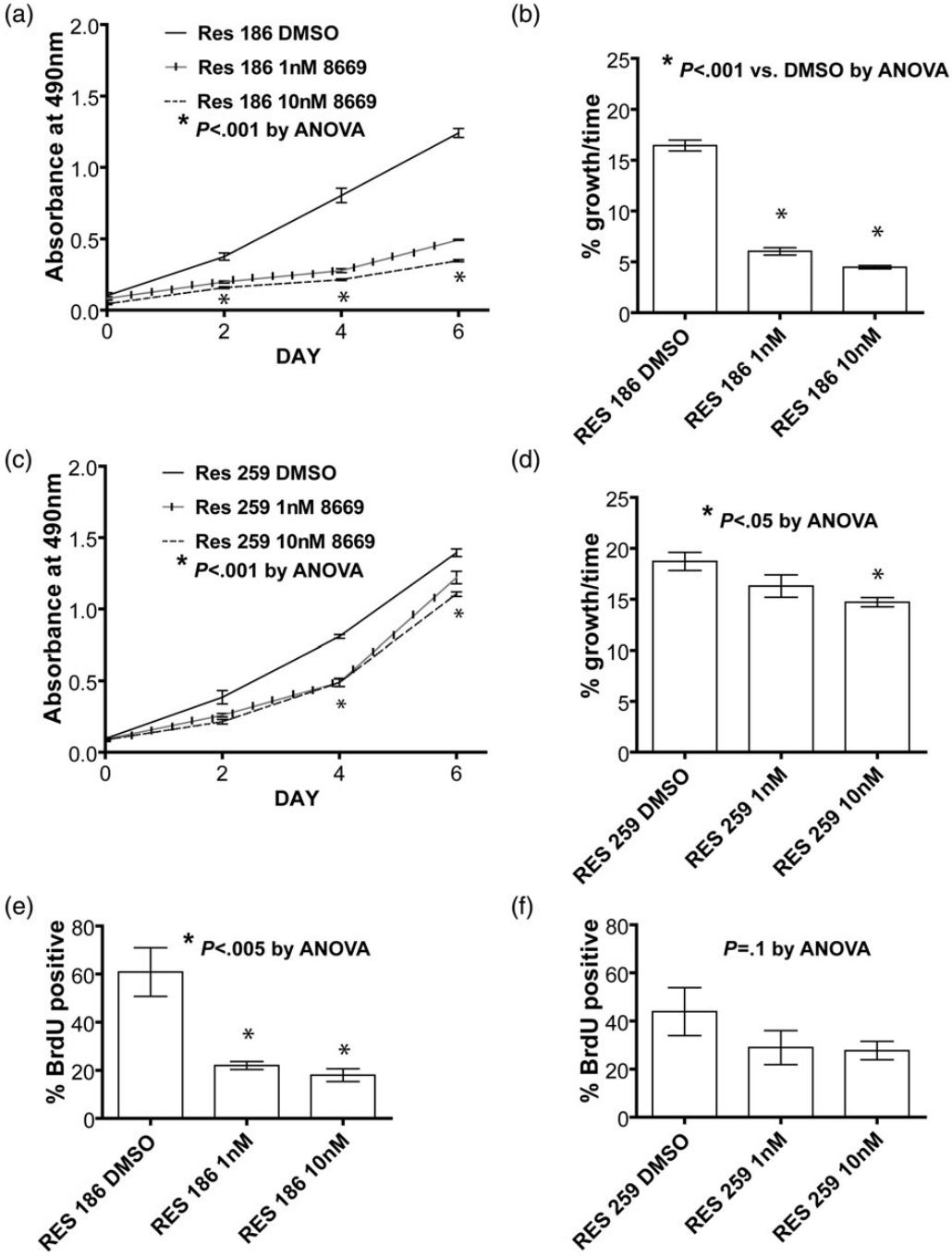

Fig. 5. mTORC1 inhibition inhibits growth and proliferation in PLGG cell lines Res186 and Res259. Growth curves from an MTS experiment and histograms showing percent change in cell growth of low-grade glioma cell lines when treated with an mTORC1 inhibitor. (**a,b,e**) Res186 is very sensitive to MK8669 treatment, as shown by the decrease in growth and decreased BrdU incorporation starting at a low drug concentration. (**c,d,f**) Res259 shows a more modest decrease in cell growth and a more modest attenuation of proliferation when treated with MK8669. Cells in this experiment were grown in media with 2% fetal bovine serum.

found *PTEN* promoter methylation in most PLGGs and in half of grade I tumors, supporting a possible role for epigenetic regulation of mTOR pathway activity in a subset of sporadic PAs as well. Furthermore, a recent microRNA profiling study showed differential overexpression of miR-21 and miR-23a in PA compared with nonneoplastic brain.[29] These microRNAs may facilitate tumorigenesis in part by targeting PTEN.[30,31] All these findings support a role for mTOR signaling in the biology of sporadic PA.

One of the main limitations of studying PLGG biology is the relative paucity of in vitro and in vivo models compared with high-grade gliomas. Although BRAF activation is relevant to low-grade gliomagenesis in vivo,[32] an important limiting factor is the phenomenon of

oncogene-induced senescence, a known effect of introducing activated *BRAF*.[21,33] Given the relative lack of PLGG cell lines, we chose lines Res186 and Res259 for our experiments, obtained from pediatric PA and diffuse (grade II) astrocytoma, respectively.[20] Although these lines contain genetic alterations that are relatively rare in PLGG (homozygous *PTEN* deletion in Res186, and *PDGFRA* gain and *CDKN2A* deletion in Res259), they proliferate well in culture, which facilitates functional experiments. Both of these cell lines show increased activation of MEK/extracellular signal-regulated kinase, which is a hallmark of PLGG.[20,34] We found that growth of Res186 and Res259 was suppressed by the mTORC1 inhibitor MK8669. Increased Akt activation, as demonstrated by pAkt (Ser473), was observed after mTORC1 inhibition, consistent with prior observations of increased mTORC2 activation after mTORC1 inhibition through loss of a negative inhibitory signaling loop.[13] Res186 (PA-derived) showed greater growth suppression than Res259 upon mTORC1 inhibition; in addition to growth suppression, Res186 cells had decreased S-phase entry after MK8669, as determined by BrdU incorporation. Susceptibility to mTOR inhibition in Res186 cells could potentially be attributed to a reliance on the PI3K/Akt/mTOR pathway, due to its *PTEN* deletion, which constitutively activates Akt.[20] Conversely, resistance to mTOR inhibition in Res259 could be due to its higher grade and therefore more complex genome, whose alterations may aid in bypassing inhibition of this particular pathway. Furthermore, this raises the possibility that different PLGG subsets demonstrate differential susceptibility to pharmacologic mTOR inhibition.

Of relevance to the cell lines we selected, we have previously shown that *PTEN* and *CDKN2A* deletions, as well as increased Akt/mTOR pathway activation, are found to an increased frequency in PA with aggressive histologic features.[16] Other groups have confirmed the association of *CDKN2A* loss with worse prognosis in PLGG.[35] This suggests that several genetic alterations are required for low-grade gliomas to bypass senescence and grow successfully in vitro.

In summary, our study demonstrates activation of both mTORC1 and mTORC2 signaling in the majority of PLGGs while highlighting heterogeneity amongst entities, anatomic locations, and NF1 status in regard to activation of mTORC1 and/or mTORC2. This heterogeneity suggests that PLGGs may not respond equally to rapalogs targeting mTORC1, such as everolimus, which is currently in clinical trials for PLGGs in children and adults (clinical trials.gov identifiers NCT01158651, NCT00782626, NCT00823459, and NCT00831324). Pending on the results of these trials, our in vitro data support the notion that inhibition of mTORC1 could be an effective therapeutic strategy for low-grade glioma. Given the large sample size and comprehensive analysis of both mTORC1 and mTORC2 pathway signaling components, our study results should aid in the design of candidate biomarker studies[36] on formalin-fixed/paraffin-embedded PLGG tissue in conjunction with future clinical trials with agents targeting specific components of the mTORC pathway.

Supplementary Material

Supplementary material is available online at *Neuro-Oncology* (http://neuro-oncology.oxfordjournals.org/).

Funding

Funding was provided by the Childhood Brain Tumor Foundation (to F.J.R.), the PLGA Foundation (to C.G.E.), the Pilocytic/Pilomyxoid Fund (to C.G.E., F.J.R.), the Knights Templar Eye Foundation (to E.H.R.), and Ian's Friend Foundation (to M.A.K.). E.H.R. is a St. Baldrick's Scholar.

Acknowledgments

The authors thank Jessica Hicks and Dr Alan Meeker from the immunohistochemistry core at Johns Hopkins, and Yasmeen Sarfraz and Faisal Huq Ronny (NYU) for excellent technical assistance, as well as Dr Chris Jones (Sutton, United Kingdom) for kindly providing cell lines Res186 and Res259.

Conflict of interest statement. None declared.

References

1. Sievert AJ, Fisher MJ. Pediatric low-grade gliomas. *J Child Neurol*. 2009;24(11):1397–1408.
2. Kluwe L, Hagel C, Tatagiba M, et al. Loss of NF1 alleles distinguish sporadic from NF1-associated pilocytic astrocytomas. *J Neuropathol Exp Neurol*. 2001;60(9):917–920.
3. Bar EE, Lin A, Tihan T, Burger PC, Eberhart CG. Frequent gains at chromosome 7q34 involving BRAF in pilocytic astrocytoma. *J Neuropathol Exp Neurol*. 2008;67(9):878–887.
4. Jones DT, Kocialkowski S, Liu L, et al. Tandem duplication producing a novel oncogenic BRAF fusion gene defines the majority of pilocytic astrocytomas. *Cancer Res*. 2008;68(21):8673–8677.
5. Pfister S, Janzarik WG, Remke M, et al. BRAF gene duplication constitutes a mechanism of MAPK pathway activation in low-grade astrocytomas. *J Clin Invest*. 2008;118(5):1739–1749.
6. Sievert AJ, Jackson EM, Gai X, et al. Duplication of 7q34 in pediatric low-grade astrocytomas detected by high-density single-nucleotide polymorphism-based genotype arrays results in a novel BRAF fusion gene. *Brain Pathol*. 2009;19(3):449–458.
7. Jones DT, Kocialkowski S, Liu L, Pearson DM, Ichimura K, Collins VP. Oncogenic RAF1 rearrangement and a novel BRAF mutation as alternatives to KIAA1549:BRAF fusion in activating the MAPK pathway in pilocytic astrocytoma. *Oncogene*. 2009;28(20):2119–2123.

8. Forshew T, Tatevossian RG, Lawson AR, et al. Activation of the ERK/MAPK pathway: a signature genetic defect in posterior fossa pilocytic astrocytomas. *J Pathol*. 2009;218(2):172–181.
9. Rodriguez FJ, Ligon AH, Horkayne-Szakaly I, et al. BRAF duplications and MAPK pathway activation are frequent in gliomas of the optic nerve proper. *J Neuropathol Exp Neurol*. 2012;71(9):789–794.
10. Ramkissoon LA, Horowitz PM, Craig JM, et al. Genomic analysis of diffuse pediatric low-grade gliomas identifies recurrent oncogenic truncating rearrangements in the transcription factor MYBL1. *Proc Natl Acad Sci U S A*. 2013;110:8188–8193.
11. Zhang J, Wu G, Miller CP, et al. Whole-genome sequencing identifies genetic alterations in pediatric low-grade gliomas. *Nat Genet*. 2013; 45:602–612.
12. Akhavan D, Cloughesy TF, Mischel PS. mTOR signaling in glioblastoma: lessons learned from bench to bedside. *Neuro Oncol*. 2010;12(8):882–889.
13. Guertin DA, Sabatini DM. The pharmacology of mTOR inhibition. *Sci Signal*. 2009;2(67):pe24.
14. Banerjee S, Crouse NR, Emnett RJ, Gianino SM, Gutmann DH. Neurofibromatosis-1 regulates mTOR-mediated astrocyte growth and glioma formation in a TSC/Rheb-independent manner. *Proc Natl Acad Sci U S A*. 2011;108(38):15996–16001.
15. Jentoft M, Giannini C, Cen L, et al. Phenotypic variations in NF1-associated low grade astrocytomas: possible role for increased mTOR activation in a subset. *Int J Clin Exp Pathol*. 2010;4(1):43–57.
16. Rodriguez EF, Scheithauer BW, Giannini C, et al. PI3K/AKT pathway alterations are associated with clinically aggressive and histologically anaplastic subsets of pilocytic astrocytoma. *Acta Neuropathol*. 2011;121(3): 407–420.
17. Kaul A, Chen YH, Emnett RJ, Dahiya S, Gutmann DH. Pediatric glioma-associated KIAA1549:BRAF expression regulates neuroglial cell growth in a cell type-specific and mTOR-dependent manner. *Genes Dev*. 2012;26(23):2561–2566.
18. Franz DN, Belousova E, Sparagana S, et al. Efficacy and safety of everolimus for subependymal giant cell astrocytomas associated with tuberous sclerosis complex (EXIST-1): a multicentre, randomised, placebo-controlled phase 3 trial. *Lancet*. 2013;381(9861):125–132.
19. Lin A, Rodriguez FJ, Karajannis MA, et al. BRAF alterations in primary glial and glioneuronal neoplasms of the central nervous system with identification of 2 novel KIAA1549:BRAF fusion variants. *J Neuropathol Exp Neurol*. 2012;71(1):66–72.
20. Bax DA, Little SE, Gaspar N, et al. Molecular and phenotypic characterisation of paediatric glioma cell lines as models for preclinical drug development. *PLoS One*. 2009;4(4):e5209.
21. Raabe EH, Lim KS, Kim JM, et al. BRAF activation induces transformation and then senescence in human neural stem cells: a pilocytic astrocytoma model. *Clin Cancer Res*. 2011;17(11):3590–3599.
22. Tchoghandjian A, Fernandez C, Colin C, et al. Pilocytic astrocytoma of the optic pathway: a tumour deriving from radial glia cells with a specific gene signature. *Brain*. 2009;132(Pt 6):1523–1535.
23. Lee da Y, Yeh TH, Emnett RJ, White CR, Gutmann DH. Neurofibromatosis-1 regulates neuroglial progenitor proliferation and glial differentiation in a brain region-specific manner. *Genes Dev*. 2010;24(20):2317–2329.
24. Krueger DA, Care MM, Holland K, et al. Everolimus for subependymal giant-cell astrocytomas in tuberous sclerosis. *N Engl J Med*. 2010;363(19):1801–1811.
25. Bettegowda C, Agrawal N, Jiao Y, et al. Exomic sequencing of four rare central nervous system tumor types. *Oncotarget*. 2013;4(4):572–583.
26. Schindler G, Capper D, Meyer J, et al. Analysis of BRAF V600E mutation in 1,320 nervous system tumors reveals high mutation frequencies in pleomorphic xanthoastrocytoma, ganglioglioma and extra-cerebellar pilocytic astrocytoma. *Acta Neuropathol*. 2011;121(3):397–405.
27. Sievert AJ, Lang SS, Boucher KL, et al. Paradoxical activation and RAF inhibitor resistance of BRAF protein kinase fusions characterizing pediatric astrocytomas. *Proc Natl Acad Sci U S A*. 2013;110(15):5957–5962.
28. Mueller S, Phillips J, Onar-Thomas A, et al. PTEN promoter methylation and activation of the PI3K/Akt/mTOR pathway in pediatric gliomas and influence on clinical outcome. *Neuro Oncol*. 2012;14(9):1146–1152.
29. Ho CY, Bar E, Giannini C, et al. MicroRNA profiling in pediatric pilocytic astrocytoma reveals biologically relevant targets, including PBX3, NFIB, and METAP2. *Neuro Oncol*. 2013;15(1):69–82.
30. Ma X, Kumar M, Choudhury SN, et al. Loss of the miR-21 allele elevates the expression of its target genes and reduces tumorigenesis. *Proc Natl Acad Sci U S A*. 2011;108(25):10144–10149.
31. Tan X, Wang S, Zhu L, et al. cAMP response element-binding protein promotes gliomagenesis by modulating the expression of oncogenic microRNA-23a. *Proc Natl Acad Sci U S A*. 2012;109(39):15805–15810.
32. Gronych J, Korshunov A, Bageritz J, et al. An activated mutant BRAF kinase domain is sufficient to induce pilocytic astrocytoma in mice. *J Clin Invest*. 2011;121(4):1344–1348.
33. Jacob K, Quang-Khuong DA, Jones DT, et al. Genetic aberrations leading to MAPK pathway activation mediate oncogene-induced senescence in sporadic pilocytic astrocytomas. *Clin Cancer Res*. 2011;17(14): 4650–4660.
34. Tatevossian RG, Lawson AR, Forshew T, Hindley GF, Ellison DW, Sheer D. MAPK pathway activation and the origins of pediatric low-grade astrocytomas. *J Cell Physiol*. 2010;222(3):509–514.
35. Horbinski C, Nikiforova MN, Hagenkord JM, Hamilton RL, Pollack IF. Interplay among BRAF, p16, p53, and MIB1 in pediatric low-grade gliomas. *Neuro Oncol*. 2012;14(6):777–789.
36. Liao YM, Sy A, Yen Y. Markers for efficacy of mammalian target of rapamycin inhibitor. *Anticancer Res*. 2012;32(10):4235–4244.